Heteroatoms-doped carbon materials with interconnected channels as ultrastable anodes for lithium/sodium ion batteries

Zhiqiang Li,[a,b] Le Cai,[a,b] Kainian Chu,[a,b] Shikai Xu,[a,b] Ge Yao,[a,b] Lingzhi Wei[a,b] and Fangcai Zheng*[a,b]

[a] Institutes of Physical Science and Information Technology, Anhui University, Hefei 230601, China

[b] Key Laboratory of Structure and Functional Regulation of Hybrid Materials, Anhui University, Ministry of Education, Hefei 230601, China

* zfcai@mail.ustc.edu.cn. Z. Q. Li and L. Cai are co-first authors for this work.

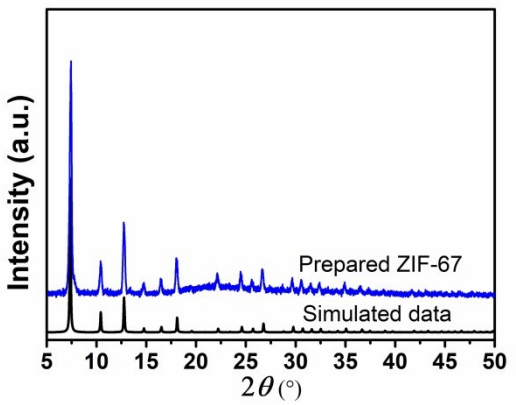

Figure S1. Experimental and simulated XRD patterns of as-prepared ZIF-67 polyhedrons.

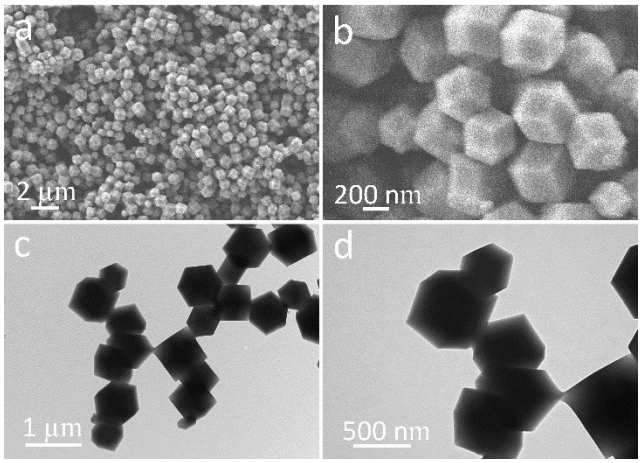

Figure S2. (a, b) SEM and (c, d) TEM images of as-prepared ZIF-67 polyhedrons.

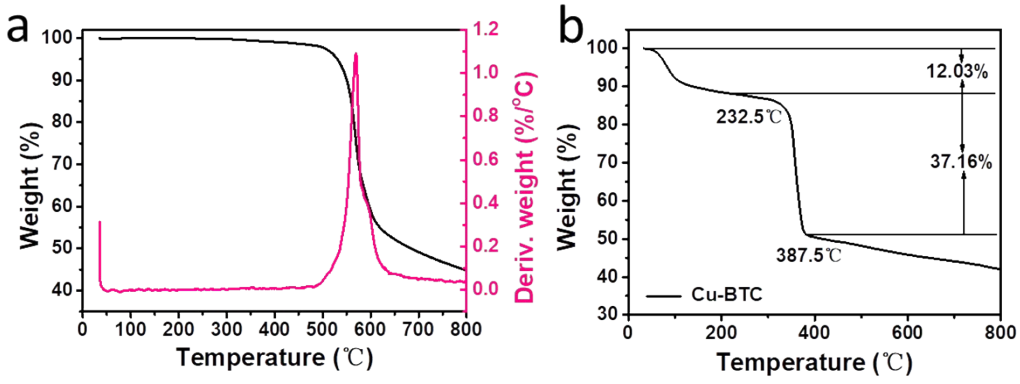

Figure S3. TGA curves of as-prepared (a) ZIF-67 polyhedrons and (b)Cu-BTC in N_2.

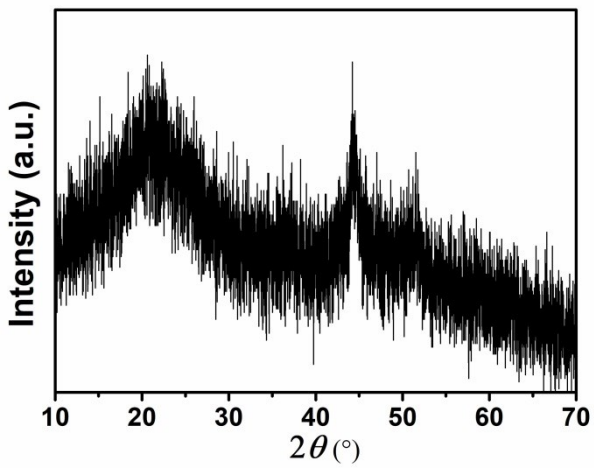

Figure S4. XRD pattern of Co nanoparticles embedded in simultaneously generated carbon matrix.

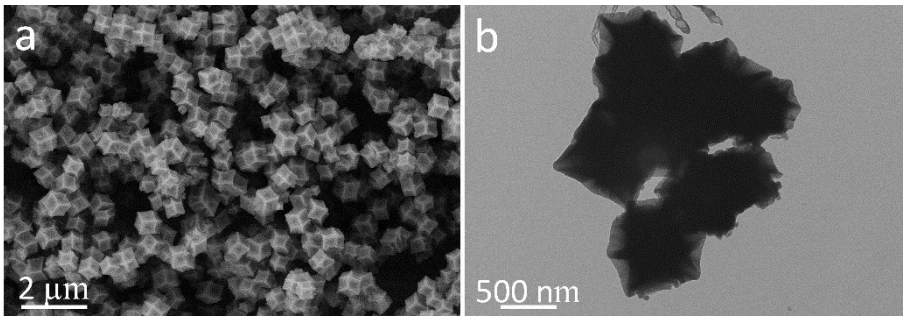

Figure S5. (a) SEM and (b) TEM images of Co nanoparticles embedded in simultaneously generated carbon matrix.

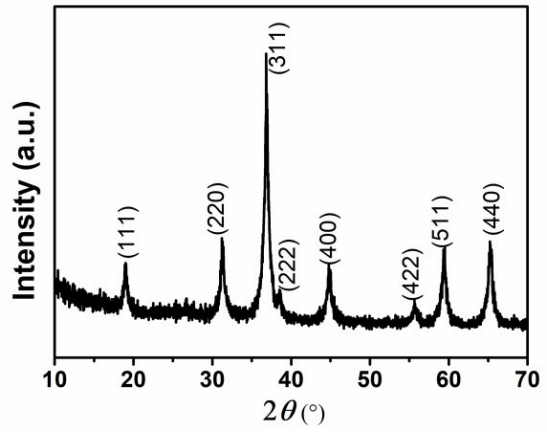

Figure S6. XRD pattern of Co_3O_4 nanoparticles embedded in porous carbon matrix.

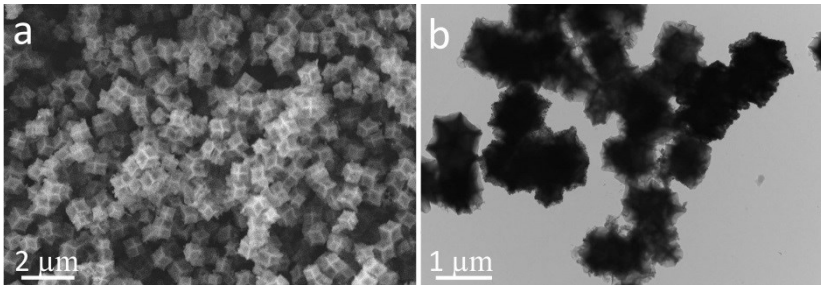

Figure S7. (a) SEM and (b) TEM images of Co_3O_4 nanoparticles embedded in porous carbon matrix.

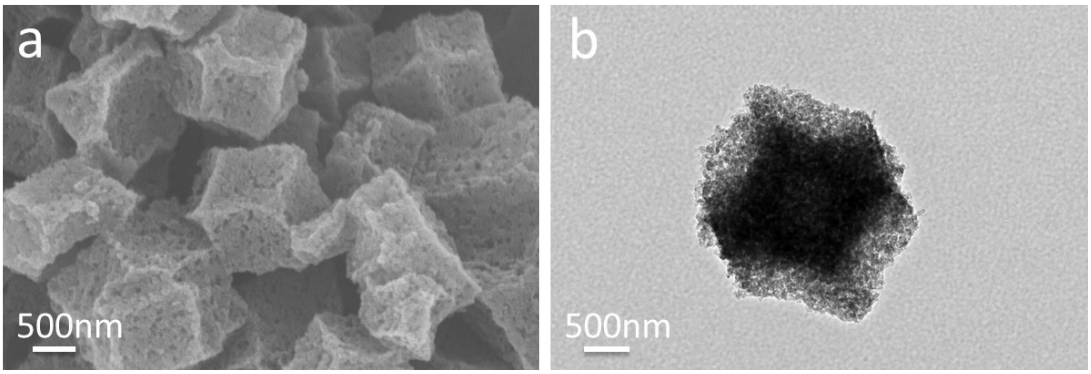

Figure S8. (a) SEM and (b) TEM images of NOPCP-700.

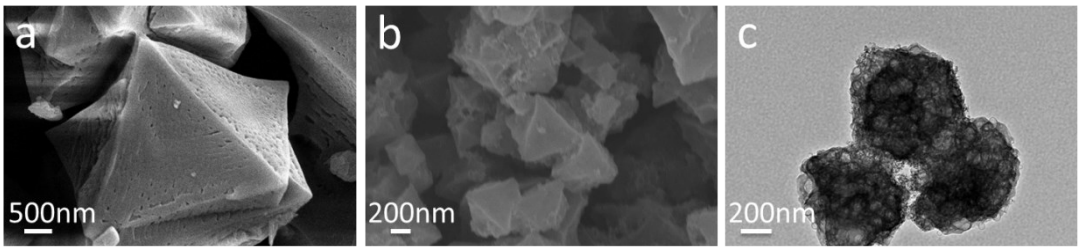

Figure S9. SEM images of (a) Cu-BTC and (b) PCP, (c) TEM image of PCP.

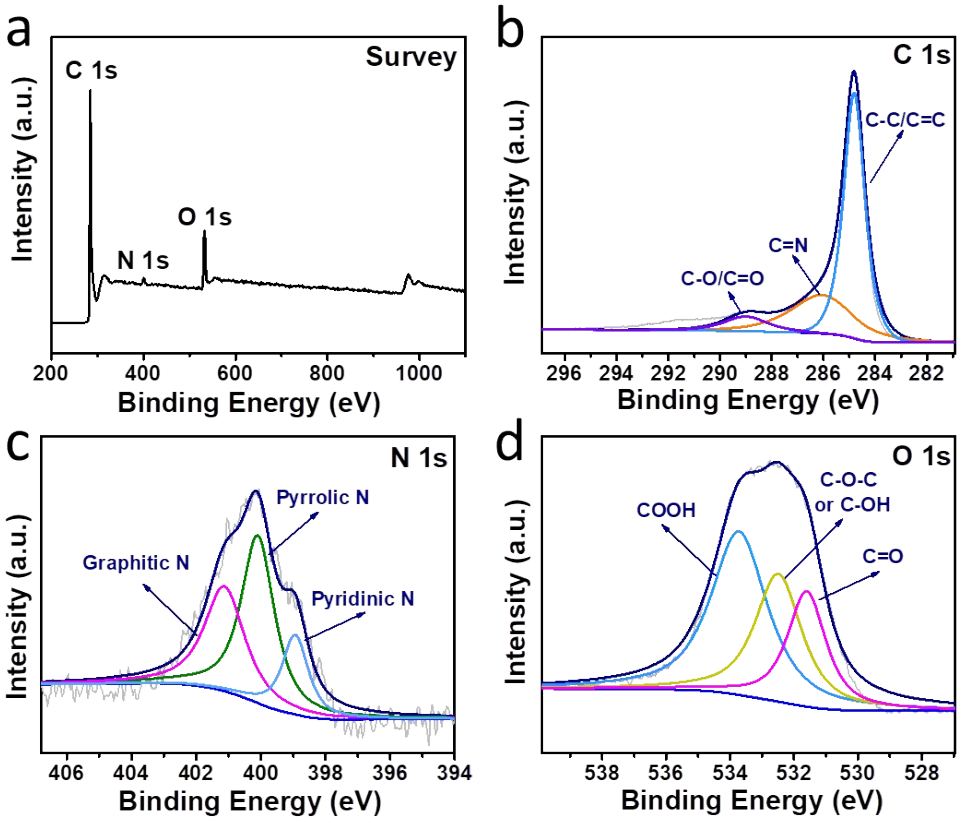

Figure S10. (a) Survey XPS spectrum, and high-resolution XPS spectra of (c) C 1s, (c) N 1s, and (d) O 1s for NOPCP-700.

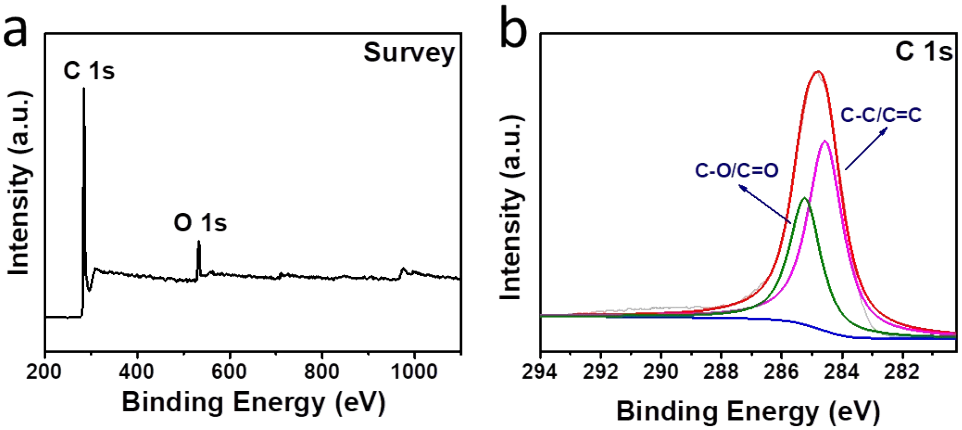

Figure S11. (a) Survey XPS spectrum, and (b) high-resolution XPS spectra of C 1s for PCP.

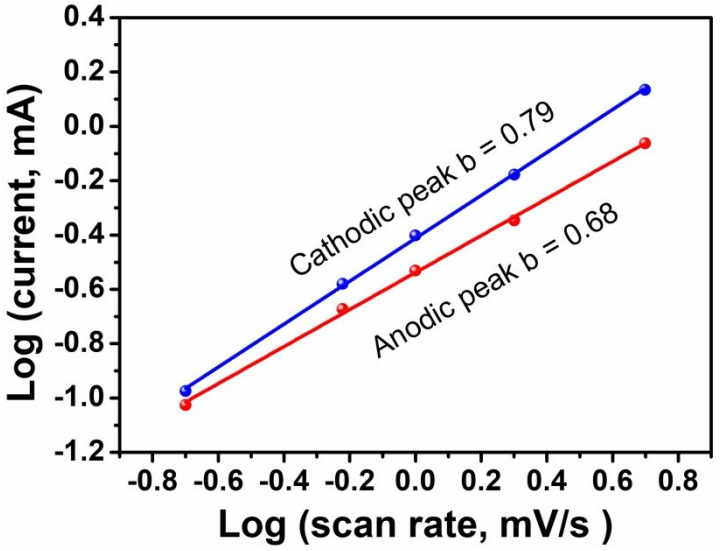

Figure S12. The b-value determination of NOPCP-600 for LIBs.

.

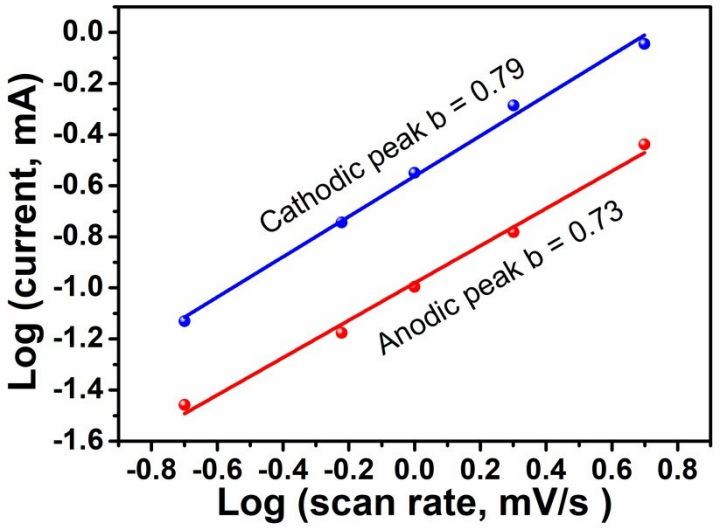

Figure S13. The b-value determination of NOPCP-600 for SIBs.

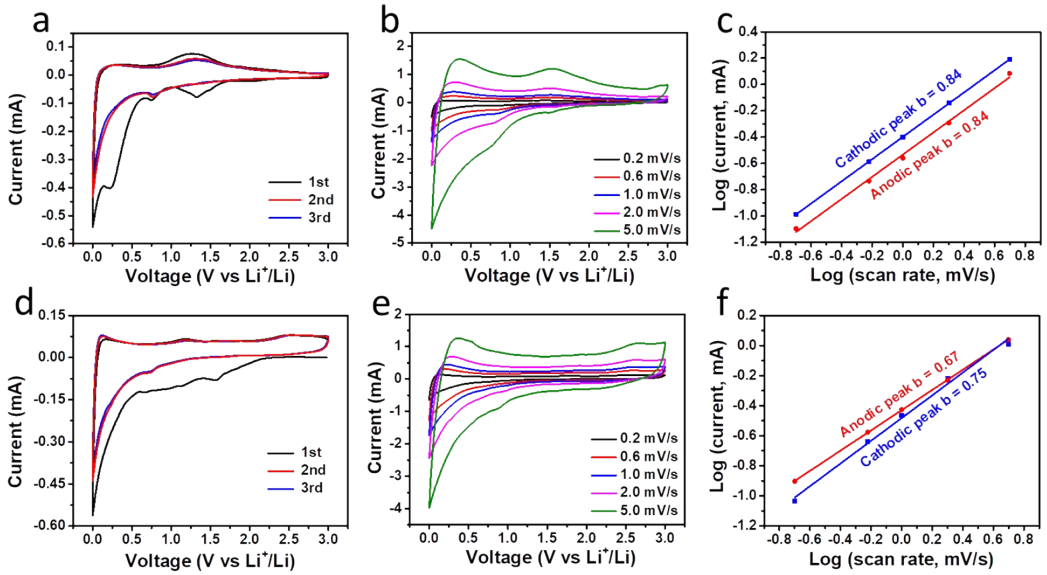

Figure S14. Electrochemical kinetic analysis of PCP and NOPCP-700 in LIBs (a and d) CV curves over a voltage range of 0.01-3.0 V at a scan rate of 0.1 mV s^{-1}, (b and e) CV curves at various scan rate, (c and f) the b-value determination for LIBs.

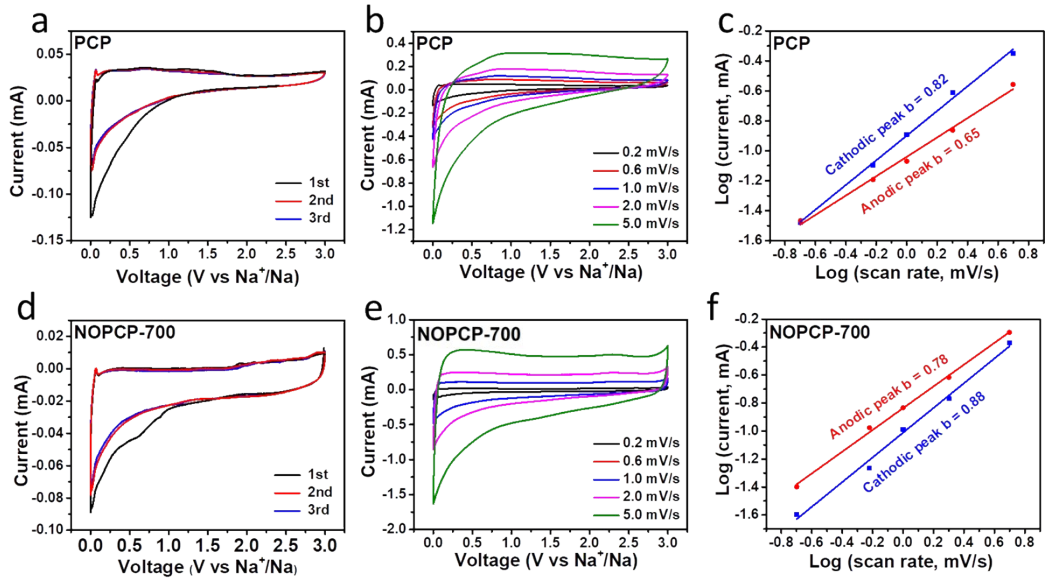

Figure S15. Electrochemical kinetic analysis of PCP and NOPCP-700 in SIBs (a and d) CV curves over a voltage range of 0.01-3.0 V at a scan rate of 0.1 mV s^{-1}, (b and e) CV curves at various scan rate, (c and f) the b-value determination for SIBs.

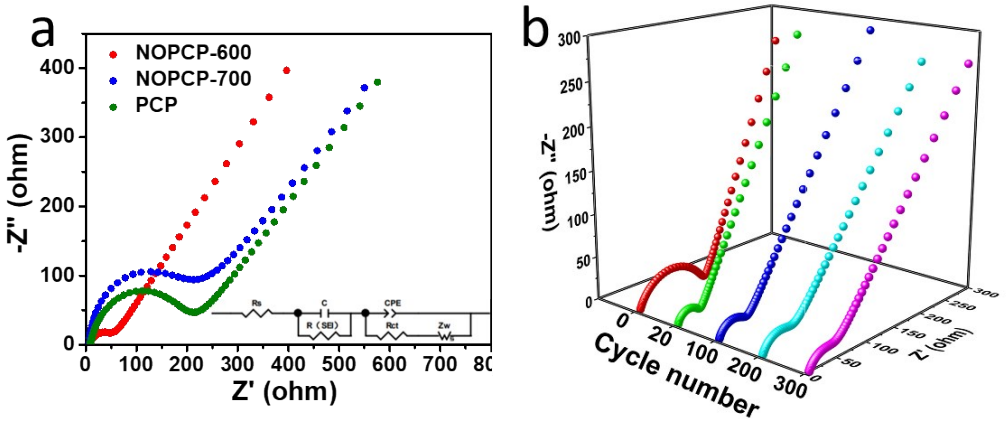

Figure S16. Nyquist plots of (a) NOPCP-600, NOPCP-700, PCP acquired at the 200th at a current density of 500 mA g^{-1} between 0.01 and 3 V for LIBs and (b) NOPCP-600 acquired at the 1th, 20th, 100th, 200th, and 300th cycles.

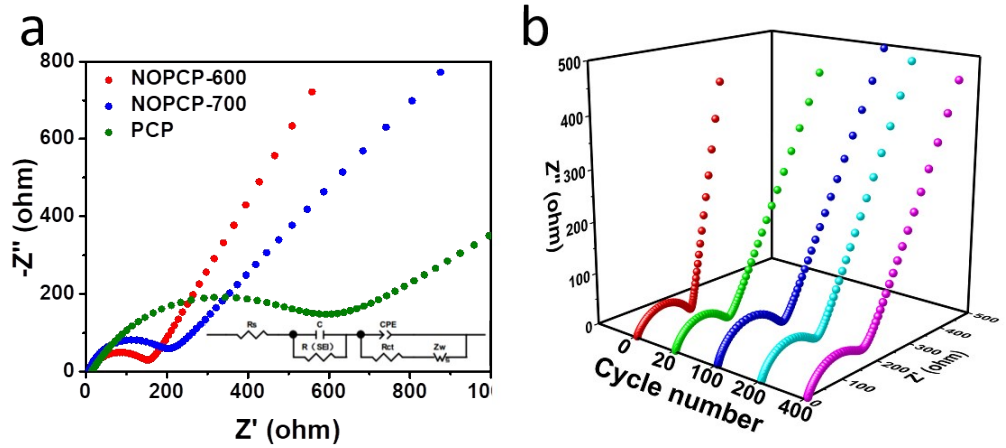

Figure S17. Nyquist plots of a) NOPCP-600, NOPCP-700, PCP acquired at the 200th at a current density of 500 mA g^{-1} between 0.01 and 3 V for SIBs and (b) NOPCP-600 acquired at the 1th, 20th, 100th, 200th, and 400th cycles.

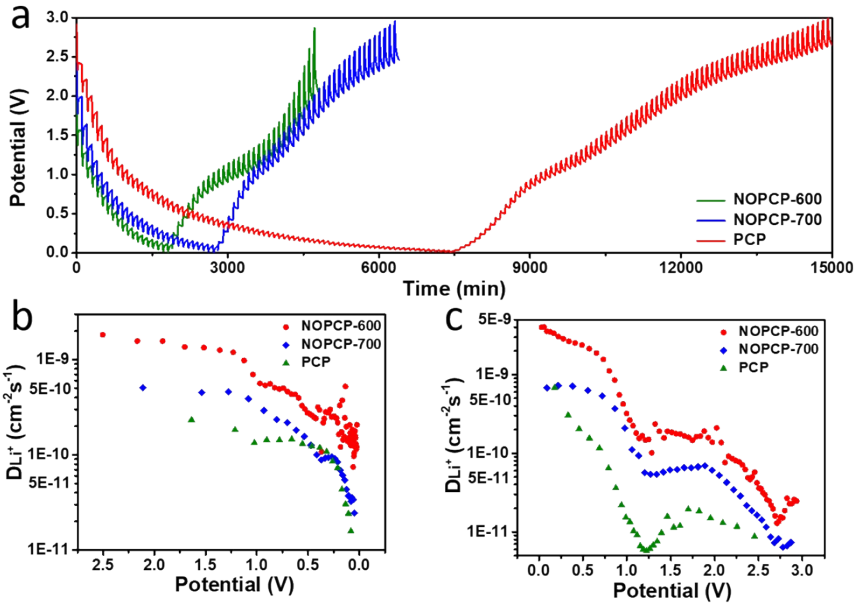

Fig. S18 (a) GITT curves and (b and c) the corresponding Li^+ diffusion coefficient of NOPCP-600, NOPCP-700 andPCP electrodes in the discharge process and charge process.

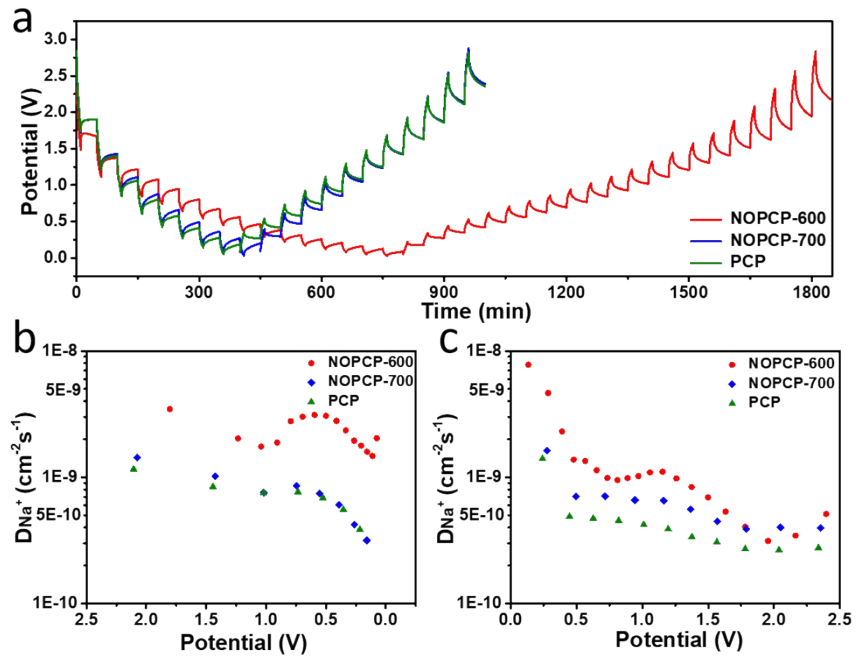

Fig. S19 (a) GITT curves and (b and c) the corresponding Na^+ diffusion coefficient of NOPCP-600, NOPCP-700 andPCP electrodes in the discharge process and charge process.

Table S1. Comparison of the lithium-storage capacity of this work with the reported ones for carbon materials.

Samples	Current density (mA g^{-1})	Cycle number	initial coulombic efficiency	Capacity (mAh g^{-1})	Ref.
N-doped carbon	100	100	53.0% （100 mA g^{-1}）	1870	S1
	1000	100		1150	
N-doped grapheme-like carbon	50	200	50.3% (50 mA g^{-1})	1143	S2
N-GCNs	100	100	53.4% (100mA g^{-1})	1236	S3
Porous carbon sheets	100	130	47.6% (100 mA g^{-1})	1467	S4
	1000	2000		710	
Three-dimensional porous carbon	100	150	64.9% （100 mA g^{-1}）	941	S5
	2000	1000		469.2	
N-doped carbon framework	1000	1000	64.99% (100 mA g^{-1})	596.1	S6
MOF-derive N-doped carbon	1000	500	45.2% (1000 mA g^{-1})	609	S7
NOPCP	100	120	56.85%	1663	This

	2000	1000	(100 mA g^{-1})	667	work

Table S2. Comparison of the sodium-storage capacity of this work with the reported one for carbon materials.

Samples	Current density (mA g^{-1})	Cycle number	initial coulombic efficiency	Capacity (mAh g^{-1})	Ref.
HCONs-500	100	100	45% (0.1A g^{-1})	262	S8
HCNFs	100	450	70.4% (0.1A g^{-1})	266	S9
	1600	5000		85	
PC-3	100	200	63.9% (0.1A g^{-1})	310.4	S10
NCNFs-IWNC800	100	350	57% (0.1A g^{-1})	278	S11
	10000	5000		148	
N-HC	200	200	51.15% (50 mA g^{-1})	214	S12
3DPC	50	100	40% (50 mA g^{-1})	284	S13
3DHPCM	50	300	62.2% (50 mA g^{-1})	281	S14
	500	3000		175	
NOHPHC	500	4000	32.6% (500 mA g^{-1})	184	S15
NOPCP	100	100	30.41% (100 mA g^{-1})	313	This work
	1000	2000		228	

Referrences

[1] J. Y. Jin, Z. W. Wang, R. Wang, J. L. Wang, Z. D. Huang, Y. W. Ma, H. Li, S. H. Wei, X. Huang, J. X. Yan, S. Z. Li and W. Huang, *Adv. Funct. Mater.*, 2019, **29**, 1807441.

[2] Y. H. Tang, J. J. Chen, X. Wang, X. X. Wang, Y. Zhao, Z. Y. Mao and D. J.

Wang, *Electrochimica Acta*, 2019, **324**, 134880.

[3] S. F. Huang, Z. P. Li, B. Wang, J. J. Zhang, Z. Q. Peng, R. J. Qi, J. Wang and Y. F. Zhao, *Adv. Funct. Mater.*, 2018, **28**, 1706294.

[4] F. Sun, K. F. Wang, L. J. Wang, T. Pei, J. H. Gao, G. B. Zhao and Y. F. Lu, *Carbon*, 2019, **155**, 166-175.

[5] H. H. Wei, K. X. Liao, P. H. Shi, J. C. Fan, Q. J. Xu and Y. L. Min, *Nanoscale*, 2018, **10**, 15842-15853.

[6] J. R. Wang, H. B. Fan, Y. M. Shen, C. P. Li and G. Wang, *Chem. Eng. J.*, 2019, **357**, 376-383.

[7] X. G. Han, L. M. Sun, F. Wang and D. Sun, *J. Mater. Chem. A*, 2018, **6**, 18891-18897.

[8] S. T. Liu, B. B. Yang, J. H. Zhou and H. H. Song, *J. Mater. Chem. A*, 2019, **7**, 18499-18509.

[9] H. X. Han, X. Y. Chen, J. F. Qian, F. P. Zhong, X. M. Feng and W. H. Chen, X. P. Ai, H. X. Yang, Y. L. Cao, *Nanoscale*, 2019, **11**, 21999-22005.

[10] Y. D. Zhu, Y. Huang, C. Chen, M. Y. Wang and P. B. Liu, *Electrochimica Acta*, 2019, **321**, 134698.

[11] W. X. Zhao, X. Hu, S. Q. Ci, J. X. Chen, G. X. Wang, Q. H. Xu and Z. H. Wen, *Small*, 2019, **15**, 1904054.

[12] X. D. Hu, X. H. Sun, S. J. Yoo, B. Evanko, F. Fan, S. Cai, C. M. Zheng, W. B. Hu and G. D. Stucky, *Nano Energy*, 2019, **56**, 828-839.

[13] X. Y. Gao, G. Zhu, X. J. Zhang and T. Hu, *Micropor. Mesopor. Mat.*, 2019, **273**, 156-162.

[14] J. Gong, G. Q. Zhao, J. K. Feng, G. L. Wang, Y. L. An, L. Zhang and B. Li, *ACS Appl. Mater. Interfaces*, 2019, **11**, 9125-9135.

[15] M. Huang, B. J. Xi, Z. Y. Feng, J. Liu, J. K. Feng, Y. T. Qian and S. L. Xiong, *J. Mater. Chem. A*, 2018, **6**, 16465-16474.